Vibration spectra of single atomic nanocontacts

2006 J. Phys.: Condens. Matter 18 8683

(http://iopscience.iop.org/0953-8984/18/39/001)

INSTITUTE OF PHYSICS PUBLISHING JOURNAL OF PHYSICS: CONDENSED MATTER

J. Phys.: Condens. Matter **18** (2006) 8683–8691 doi:10.1088/0953-8984/18/39/001

Vibration spectra of single atomic nanocontacts

B Bourahla[1,2,4], **A Khater**[2,3,4], **O Rafil**[2] **and R Tigrine**[1,2]

[1] Laboratoire de Physique et Chimie Quantique, Département de Physique, Faculté des Sciences, Université Mouloud Mammeri de Tizi-Ouzou, 15000 Tizi-Ouzou, Algeria
[2] Laboratoire de Physique de l'Etat Condensé UMR 6087, Université du Maine, 72085 Le Mans, France
[3] Department of Physics, McGill University, 3600 rue University, Montreal, QC, H3A 2T8, Canada

E-mail: bourahla_boualem@yahoo.fr and antoine.khater@univ-lemans.fr

Received 29 March 2006, in final form 26 June 2006
Published 11 September 2006
Online at stacks.iop.org/JPhysCM/18/8683

Abstract

This paper introduces a simple model for an atomic nanocontact, where its mechanical properties are analysed by calculating numerically the local spectral properties at the contact atom and the nearby atoms. The standard methodology for calculating phonon spectral densities is extended to enable the calculation of localized contact modes and local density of states (DOS). The model system considered for the nanocontact consists of two sets of triple parallel semi-infinite atomic chains joined by a single atom in between. The matching method is used, in the harmonic approximation, to calculate the local Green's functions for the irreducible set of sites that constitute the inhomogeneous nanocontact domain. The Green's functions yield the vibration spectra and the DOS for the atomic sites. These are numerically calculated for different cases of elastic hardening and softening of the nanocontact domain. The purpose is to investigate how the local dynamics respond to local changes in the elastic environment. The analysis of the spectra and of the DOS identifies characteristic features and demonstrates the central role of a core subset of these sites for the dynamics of the nanocontact. The system models a situation which may be appropriate for contact atomic force microscopy.

(Some figures in this article are in colour only in the electronic version)

1. Introduction

Modern techniques can furnish nanostructures with controlled geometries as constitutive elements of mesoscopic systems. These nanostructures are potentially of technological interest in various types of devices. In particular the study of nanostructures *at surfaces* has been

[4] Authors to whom any correspondence should be addressed.

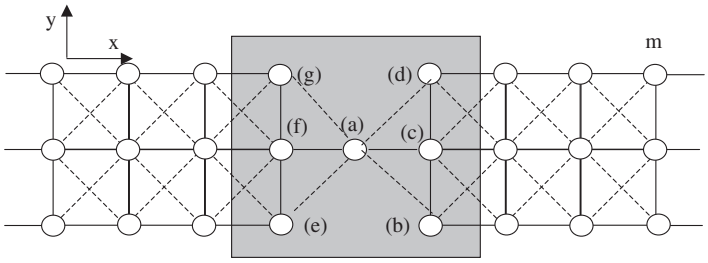

Figure 1. Schematic representation for an atomic nanocontact between quasi-one-dimensional lattice waveguides each composed of three semi-infinite chains on either side. The shaded zone denotes an effective nanocontact domain.

the subject of great efforts in recent years, and in this respect there is an increasing volume of experimental data to elucidate the structural [1–4], magnetic [5–9], and electronic [10–13] properties of quasi-one-dimensional nanostructures and monatomic chains on surfaces.

The use of such nanostructures in high technology requires a necessary basic knowledge for the adequate control of their properties. It is hence of interest to develop numerical calculations for appropriate models for these systems, notably for low-dimensional nanostructures at surfaces.

In this work, we present a simple model for the study of the vibration spectra of an atomic nanocontact which acts as a joint between two sets of semi-infinite monatomic chains. In a first approximation the system is considered to be on a solid surface with no interactions with the substrate. The system models a situation which may also be appropriate for contact force microscopy.

The paper is organized as follows. In section 2 we present the basic elements of the model, describing the dynamics and the modes of the semi-infinite group of monatomic chains. In section 3 we develop the dynamical properties of the nanocontact. The real space Green's functions that describe the nanocontact dynamics are derived and the spectral densities are also obtained. In section 4 numerical results are presented for three cases of elastic hardening and softening of the nanocontact domain, and the conclusions are given.

2. Basic elements of the model

The structural model used in this paper is presented in figure 1. It consists of two sets of triple parallel semi-infinite atomic chains. Each may be seen as an effective quasi-one-dimensional waveguide. A single atomic nanocontact serves as the joint between the two sets. The atoms are bound by elastic interactions between nearest and next nearest neighbours, in the harmonic approximation. The model is suitable for the study of the dynamics of the atomic chains on a substrate provided we can neglect the interactions between the system and the substrate. The model can also serve towards the study on a macroscopic scale of granular chains constructed in an analogous manner with linear interactions.

The elastic interactions between nearest and next nearest neighbours in the domains to the left and the right of the nanocontact are represented respectively by the constants k_1 and k_2, where the shaded area in figure 1 constitutes the effective atomic nanocontact domain. The elastic constants in this inhomogeneous boundary may differ from bulk values, and are hence labelled $k_{1\mathrm{d}}$ and $k_{2\mathrm{d}}$. It is convenient next to define the following ratios:

$$r = k_2/k_1, \qquad r_{1\mathrm{d}} = k_{1\mathrm{d}}/k_1, \qquad r_{2\mathrm{d}} = k_{2\mathrm{d}}/k_1. \tag{1}$$

The dynamics of the system are described by the equations of motion for sites l, given in the harmonic approximation by

$$\omega^2 m(l)u_\alpha(l) = -\sum_{l' \neq l}\sum_{\beta} k(l,l')d_\alpha d_\beta/d^2 \cdot [u_\beta(l) - u_\beta(l')]. \tag{2}$$

For $l = (n, m)$, the indices n and m count the sites along the x- and y-axes. α and β denote Cartesian coordinates, $m \equiv m(l)$ is the atomic mass, and $u_\alpha(l)$ the displacement vector, for l. The radius vector $\mathbf{d}$, between sites l and l', has Cartesian components d_α and $d = |\mathbf{d}|$. Note that the elastic force constants $k(l, l')$ are respectively k_1 and k_2 for nearest and next nearest neighbours.

For sites l and l' distant from the inhomogeneous boundary to the left and right of the interval $n \in [-1, 1]$ of figure 1, the equations of motion may be cast, using equation (2), in the matrix form

$$[\Omega^2 I - D(\eta, r)]|u\rangle = 0, \tag{3}$$

where $[\Omega^2 I - D(\eta, r)]$ is a 6×6 matrix, and $|u\rangle$ is the corresponding displacement vector for a column of the perfect waveguide. $D(\eta, r)$ is a dynamic matrix in the bulk of the waveguide, and I denotes a unit matrix. η is a generalized phase factor between neighbouring sites. Note that $\Omega = \omega/\omega_0$ is a dimensionless frequency, ω_0 being a characteristic lattice frequency, $\omega_0^2 = k_1/m$.

Both the propagating and the evanescent eigenmodes are described by the phase factor doublets $\{\eta, \eta^{-1}\}$. The propagating modes are determined by the condition $|\eta| = 1$, and the evanescent modes from the condition $|\eta| < 1$, [14]. The exact solutions for each doublet are obtained as a function of the normalized frequencies Ω and of the elastic and structural properties of the system. These solutions are obtained when the determinant of the secular equation of the dynamic matrix $[\Omega^2 I - D(\eta, r)]$ vanishes. For the system under study the secular equation may consequently be expressed as a polynomial:

$$\Sigma A_s \eta^s = 0. \tag{4}$$

The coefficients $A_s = A_s(\Omega, r)$ are functions of the frequency Ω and the elastic constants of the system. Due to the Hermitian nature of the dynamics, the phase factors $\{\eta, \eta^{-1}\}$ in the doublet verify symmetrically the polynomial forms, [15]. Only six of the twelve modes that are the solutions of equation (4) are, however, of physical interest. For the propagating modes η, their inverse η^{-1} are modes propagating in the opposite sense, and for the non-propagating modes only the evanescent modes $|\eta| < 1$ are considered physically.

To illustrate the model, the propagating modes for the perfect waveguides are presented in figure 2 for a choice of $r = 0.75$, as a function of the normalized wavevector $\phi_x = k_x \boldsymbol{a}$, where ϕ_x runs in the interval $[-\pi, \pi]$ over the first Brillouin zone (BZ) and $\boldsymbol{a}$ is the interatomic distance between adjacent lattice sites. The eigenmodes, labelled $i \in \{1, 2, 3, 4, 5, 6\}$, are propagating modes in the following frequency intervals:

$$\Omega_1 = [0.00, \Omega_{1,\max} = 1.30]$$
$$\Omega_2 = [0.00, \Omega_{2,\max} = 1.30]$$
$$\Omega_3 = [0.87, \Omega_{3,\max} = 1.89]$$
$$\Omega_4 = [1.28, \Omega_{4,\max} = 2.00]$$
$$\Omega_5 = [1.50, \Omega_{5,\max} = 2.20]$$
$$\Omega_6 = [2.16, \Omega_{6,\max} = 2.50].$$

There are two acoustical modes, Ω_1 and Ω_2, characterized by the limiting behaviour of their phonon branches, tending to zero frequency when the wavevector tends to zero, and four optical

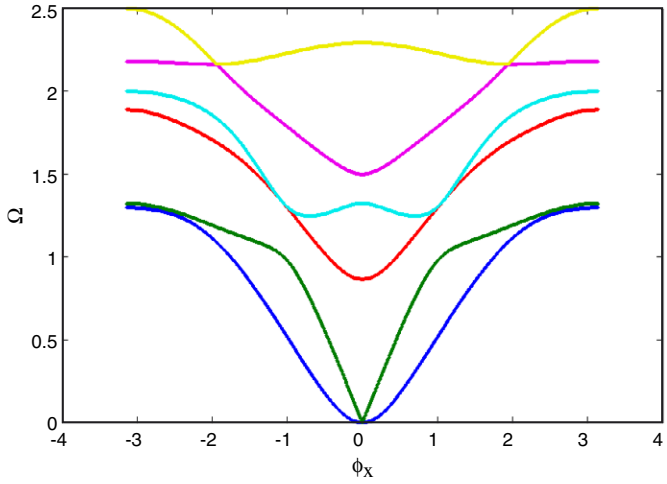

Figure 2. Typical phonon dispersion curves for the perfect quasi-one-dimensional waveguide of figure 1, for an $r = 0.75$ ratio of next nearest to nearest neighbour elastic constants. The phonon branches are presented over the first Brillouin zone of the normalized wavevector $\phi_x = k_x \boldsymbol{a}$, where ϕ_x runs in the interval $[-\pi, \pi]$.

modes with branches that differ from zero in the long-wavelength limit. Note that Ω_4 and Ω_6 start at slightly higher frequencies at the BZ centre than their minima values over their propagating intervals.

3. Nanocontact dynamics

The analysis of the dynamics of the inhomogeneous atomic nanocontact generates an infinite set of coupled equations on both sides of the atomic nanocontact. In order to render the problem tractable we need to decouple the dynamics of a representative and irreducible set of sites at the inhomogeneous boundary of the nanocontact domain from the rest of the system. This irreducible set is comprised as in figure 1 from the sites labelled (a), (b), (c), (d), (e), (f), (g), where (a) is the atomic nanocontact itself.

To decouple the infinite set of equations, the matching method procedure [14–16] is used. The displacement field u_α for an atom localized in the matching domains is hence expressed [16, 17], to the left and right of the effective nanocontact, in the analytic form

$$\begin{aligned} u_\alpha(n, m) &= \sum_{i=1}^{6} [\eta(i)]^n w(\alpha, i) R_i^+ \\ u_\alpha(n', m') &= \sum_{i=1}^{6} [\eta(i')]^{-n'} w(\alpha, i') R_{i'}^- . \end{aligned} \tag{5}$$

The factors R_i^+ and R_i^- in equations (5) represent unit vectors that span the Hilbert space of the solutions corresponding to the set of phase factors $\{\eta_i, \eta_i^{-1}\}$ for $i \in \{1, 2, 3, 4, 5, 6\}$, and the coefficients $w(\alpha, i)$ and $w(\alpha, i')$ identify the relative weighting factors associated with the atomic vibration displacements u_α and u'_α.

Denoting the basis vector in the constructed Hilbert space by $|R\rangle = |R_i^+, R_i^-\rangle$, and using equations (5) and the transformations mapping the two vectors $|R\rangle$ and $|u\rangle$, we obtain a system

of linear homogeneous equations

$$[\Omega^2 I - D_m(\eta, r)]|u, R\rangle = |0\rangle \tag{6}$$

where $[\Omega^2 I - D_m(\eta, r)]$ is a characteristic square matrix. The corresponding dimensions of this matrix (26×26) and of the vector $|u, R\rangle$ are characteristic of the irreducible set of sites in the inhomogeneous nanocontact domain.

The matching method provides a framework for the calculation of the localized modes as well as of the spectral densities. Equation (6) is the central result in this paper. By diagonalizing $[\Omega^2 I - D_m(\eta, r)]$ we are able to calculate the localized modes. In this paper, however, the results for the localized mode are not presented. Our main interest here is to calculate the spectral densities.

The most direct manner to calculate the spectral densities is via the Green's functions, which may be expressed formally [18], using equation (6), as

$$G(\Omega^2 + \mathrm{i}\varepsilon) = [(\Omega^2 + \mathrm{i}\varepsilon)I - D_m(\{\eta\}, r)]^{-1}. \tag{7}$$

The general relation for the vibration spectral matrix is given from the Green's functions by the following expression:

$$\rho^{(l,l')}_{(\alpha,\beta)}(\Omega) = -\frac{2\Omega}{\pi}\sum_m p^l_{\alpha i} p^{l'}_{\beta i}\delta(\Omega^2 - \Omega^2_m) = -\frac{2\Omega}{\pi}\lim_{\varepsilon\to 0^+}\{\mathrm{Im}[G^{ll'}_{\alpha\beta}(\Omega^2 + \mathrm{i}\varepsilon)]\} \tag{8}$$

where the quantities $p^l_{\alpha i}$ denote the α-component of the polarization vector for the atomic site l for the branch Ω_i. The spectral densities per atomic site of the effective nanocontact domain are then calculated over the trace of the matrix for $l = l'$, where l runs over the sites of the irreducible set.

The vibration density of states (DOS) per atomic site l, denoted as $N_l(\Omega)$, is obtained next as a sum over the trace of the spectral density matrix:

$$N_l(\Omega) = \sum_\alpha \rho^{(l,l)}_{(\alpha,\alpha)}(\Omega) = -\frac{2\Omega}{\pi}\sum_\alpha \lim_{\varepsilon\to 0^+}\{\mathrm{Im}[G^{ll}_{\alpha\alpha}(\Omega^2 + \mathrm{i}\varepsilon)]\}. \tag{9}$$

The vibration spectra are calculated and presented for the different sites of the nanocontact domain in the following section.

4. Numerical results and discussion

The numerical analysis is carried out for three different cases, each determining a choice of the elastic properties of the atomic nanocontact domain. These are respectively

(i)	$r = 0.75,$	$r_{1\mathrm{d}} = 0.9$	$r_{2\mathrm{d}} = 0.65.$
(ii)	$r = 0.75,$	$r_{1\mathrm{d}} = 1.0,$	$r_{2\mathrm{d}} = 0.75$
(iii)	$r = 0.75,$	$r_{1\mathrm{d}} = 1.1,$	$r_{2\mathrm{d}} = 0.85.$

The purpose of this numerical procedure is to investigate how the local dynamics respond to local changes in the elastic properties. For the atomic nanocontact domain, the first case (i) corresponds to a softening of its elastic constants in comparison to the bulk of the atomic chains, case (ii) corresponds to the situation where the elastic constants are the same as in the bulk of the atomic chains, and in contrast the third case (iii) corresponds to a hardening of its elastic constants. These possibilities are similar to situations where changes in elastic constants may take place in the neighbourhood of steps and kinks in surfaces [19]. Note that the nearest neighbour and next nearest neighbour factors, $r_{1\mathrm{d}}$ and $r_{2\mathrm{d}}$, are modified homogenously for cases (i) and (iii).

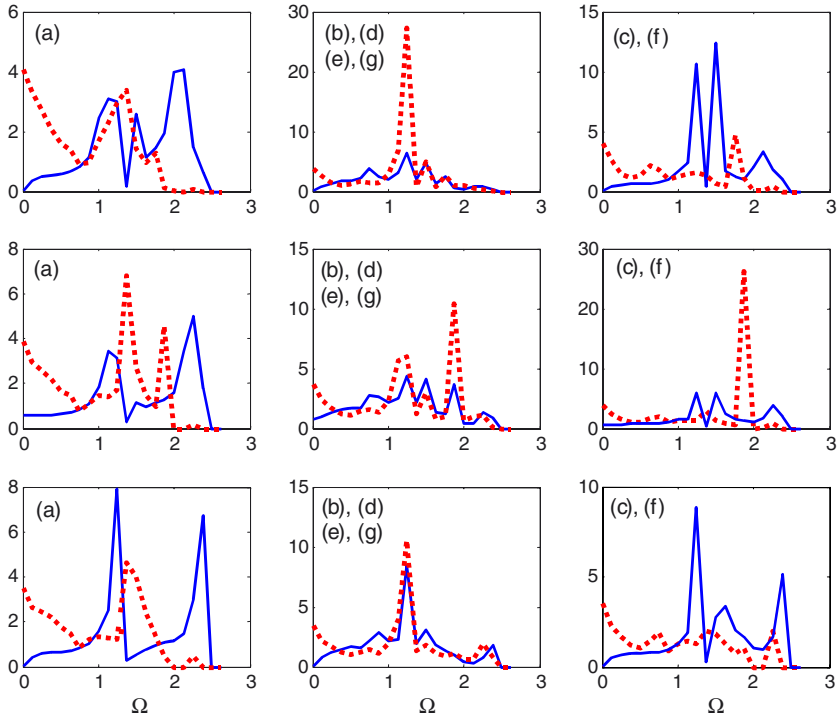

Figure 3. Spectral densities of the groups of atoms (a), then (b, d, e, g), and (c, f), of the irreducible set of sites on the effective atomic nanocontact. The spectral densities are given in arbitrary units as a function of the frequency Ω in the Brillouin zone. The results are ranged in columns per group starting with (a) at the left. The three rows from top to bottom correspond to the cases (i)–(iii) in the text. The vibration spectra along the x-axis are presented as continuous, and along the y-axis as discontinuous curves.

The vibration spectral densities are calculated numerically per atomic site for the x- and y-axes, and given in arbitrary units, as a function of the normalized frequency Ω in the Brillouin zone. The results for the spectral densities for the groups of sites (a), then (b, d, e, g), and (c, f), are presented in figure 3. The spectral densities along the x-axis are given as continuous (blue), and those along the y-axis as discontinuous (red) curves. The sites (b, d, e, g), and (c, f), present comparable structures for their spectra, consistently for each for the three cases (i), (ii) and (iii), which corresponds to evident symmetry effects.

The vibration spectral densities are ranged in columns from left to right to correspond to the groups of sites (a), then (b, d, e, g), and (c, f). The three rows from top to bottom correspond respectively to the cases (i), (ii) and (iii), indicated above. The spectra are in general sensitive to the changes of the elastic constants r_{1d} and r_{2d} in the nanocontact domain, as may be seen from figure 3. The sensitivity of these results compares to that observed for the vibration spectra at boundaries separating phase domains in hexagonal two-dimensional lattices [20].

We have also calculated the density of states (DOS), for the above sites. The numerical results are presented in figure 4, for the individual (a), (b), (c), (d), (e), (f), and (g) sites, alphabetically from top to bottom, and are arranged so that the columns from left to right correspond to the cases (i), (ii) and (iii).

There is evidence with reference to the DOS, for a localized collective resonance about $\Omega \sim 0.5$ for the ensemble of the irreducible sites of the nanocontact domain. It is observed

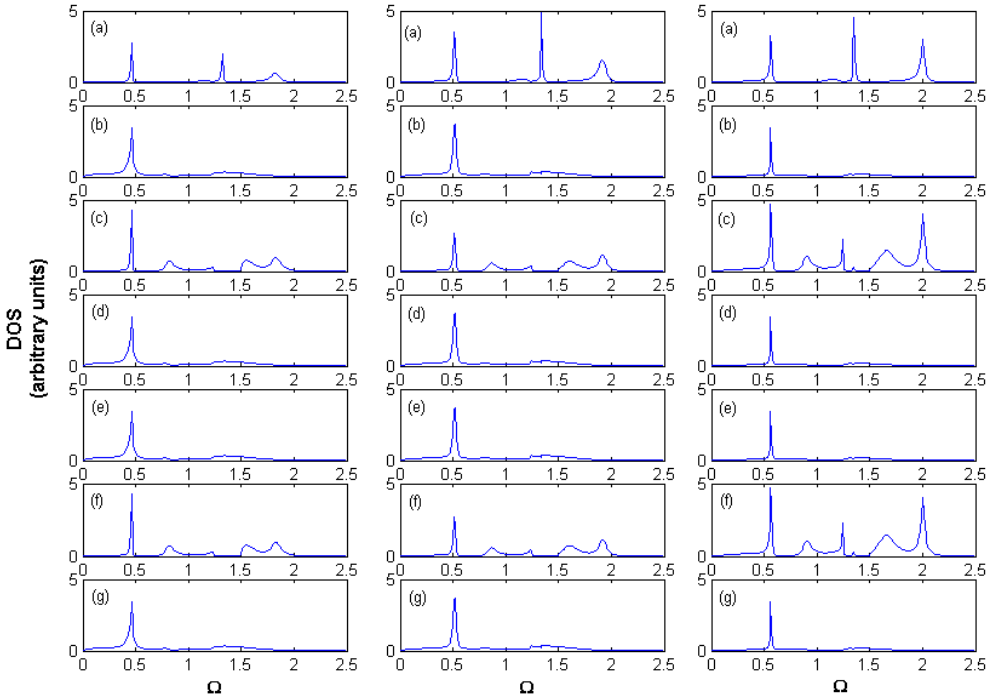

Figure 4. The densities of states (DOS) of the atoms (a), (b), (c), (d), (e), (f) and (g) of the irreducible set of sites of the atomic nanocontact, ranged from top to bottom. The columns from left to right correspond to the cases (i), (ii), and (iii), for elastic softening to hardening.

that the energy line of this mode goes to higher frequencies with increasing hardness of the elastic constants: $\Omega = 0.45$ for (i), $\Omega = 0.50$ for (ii), $\Omega = 0.55$ for (iii). The changes in Ω are of the order of magnitude of the changes considered for the elastic constants of the nanocontact domain, which leads us to the conclusion that this mode would correspond primarily to a collective vibration of the nanocontact domain in the potential well constituted *by the extremities* of the two waveguides on either side for $|n| = 2$. Apart from this mode, the corner sites (b, d, e, g) do not present any other features attesting to more of a role of confinement for the nanocontact domain.

The three sites (f, a, c) which are aligned along the principal axis of symmetry of the system, show a richer DOS than the other sites. The analysis of their DOS yields a number of further conclusions.

Site (a) presents one specific resonance line at $\Omega \approx 1.33$ that does not show up for any of the other sites. The frequency position of this mode varies little with the variations of the elastic constants in the nanocontact domain. This resonance is substantially localized on site (a). Its localized character is further attested by the spectral densities of (a) which indicate that the mode is essentially a vibration along the y-axis. This is eventually an interesting result for the use of AFM microscopy. Effectively, the spectral densities for (a) show systematically, for the cases studied, a node along the y-axis, and an antinode along the x-axis, for $\Omega \approx 1.33$.

Site (a) and sites (c, f) have next a common resonance line at $\Omega \sim 1.91$ that does not show up for any of the other sites in the nanocontact domain. The displacement of this mode towards higher frequencies with increasing elastic hardness is observed and is commensurable with the changes of the elastic constants for the three studied cases: $\Omega = 1.82$ for (i), $\Omega = 1.91$ for (ii),

$\Omega = 2.00$ for (iii). This resonance is substantially localized on sites (a, c, f). By an analysis of the spectral densities in figure 3, it is possible to argue that there is increasing interaction between sites (c, f) and site (a) as one increases the hardness of the elastic constants in the nanocontact domain, since the resonance amplitude increases monotonically. Furthermore, whereas the polarization of the mode is mixed x and y for cases (i) and (ii), it becomes substantially aligned along the x-axis for case (iii).

In contrast, the pair of sites (c, f) present three specific resonance lines that do not show up for any of the other sites in the nanocontact domain. These lines are at respectively $\Omega \sim 0.85$, $\sim$1.24, $\sim$1.55. We interpret this by assigning these resonance lines to collective localized vibration modes of the pair of sites (f, c) against the rest of the system where (a) remains stationary.

The first line is at $\Omega = 0.82$ for (i), $\Omega \sim 0.87$ for (ii), and $\Omega \sim 0.90$ for (iii); it shows a mixed x and y polarization. The third line, like the first, shows variations commensurable with the variations of the elastic constants, it is at $\Omega = 1.55$ for (i), $\Omega = 1.61$ for (ii), and $\Omega = 1.66$ for (iii); however, this line shows a predominantly x polarization throughout the domain of present interest for the elastic constants.

The second line shows minor variations: $\Omega = 1.23$ for (i), $\Omega = 1.235$ for (ii), and $\Omega = 1.24$ for (iii). The polarization of this mode is complex. It is probably orthogonal on (c) and (f), alternating rapidly as one increases the hardness.

In conclusion, we present in this work a simple model for the study of the vibration spectra of an atomic nanocontact which acts as the joint between two sets of semi-infinite monatomic chains. It enables one to address questions regarding the mechanical properties of nanocontacts. The chosen model is a generic one and it serves to demonstrate the ability of the proposed modelling and analysis tools. The analysis of the vibration spectra and of the DOS of the set of irreducible sites in the nanocontact domain demonstrates the central role of a core subset of these sites for the dynamics of the nanocontact. The model is suitable for the study of such a configuration of atomic chains on a substrate provided we can neglect the interactions between the chains and the substrate. It can also serve towards the study of granular chains constructed in an analogous manner on the classical macroscopic scale.

Acknowledgments

RT and BB would like to thank the University of Tizi-Ouzou for financial support, and the Université du Maine for their study visit. AK should also like to thank the Department of Physics at McGill for his stay, and particularly M Hilke and R Bennewitz for their discussions. We thank the referees for their useful remarks.

References

[1] Shchukin V and Bimberg D 1999 *Rev. Mod. Phys.* **71** 1125
[2] Gambardella B, Blanc M, Burgi L, Kuhnke K and Kern K 2000 *Surf. Sci.* **449** 93
[3] Kern K, Niehaus H, Schatz A, Zeppenfeld P, Goerge J and Comsa G 1991 *Phys. Rev. Lett.* **67** 855
[4] Rousset S *et al* 2002 *Mater. Sci. Eng.* B **96** 169
[5] Gambardella P, Dallmeyer A, Maiti K, Malagoli M C, Rusponi S, Ohresser P, Eberhardt W, Carbone C and Kern K 2004 *Phys. Rev. Lett.* **93** 077203
[6] Vindigni A, Rettori A, Pini M G, Carbone C and Gambardella P 2006 *Appl. Phys.* A **82** 385
[7] Weiss N, Cren T, Epple M, Rusponi S, Baudot G, Tejeda A, Repain V, Rousset S, Ohresser P, Scheurer F, Bencok P and Brune H 2005 *Phys. Rev. Lett.* **95** 157204
[8] Khater A and Abou Ghantous M 2002 *Surf. Sci. Lett.* **498** L97
[9] Abou Ghantous M and Khater A 1999 *Eur. Phys. J.* B **12**

[10] Crain J N and Pierce D T 2005 *Science* **7** 703
[11] Bürgi L, Jeandupeux O, Hirstein A, Brune H and Kern K 1998 *Phys. Rev. Lett.* **81** 5370
[12] Hasegawa Y and Avouris P 1993 *Phys. Rev. Lett.* **71** 1071
[13] Repp J, Meyer G and Rieder K H 2004 *Phys. Rev. Lett.* **92** 036803
[14] Szeftel J and Khater A 1987 *J. Phys. C: Solid State Phys.* **20** 4725
[15] Pennec Y and Khater A 1995 *Surf. Sci. Lett.* **348** 82
[16] Fellay A, Gagel F, Maschke K, Virlouvet A and Khater A 1997 *Phys. Rev.* B **55** 1707
[17] Belhadi M, Khater A, Rafil O, Hardy J and Tigrine R 2001 *Phys. Status Solidi* b **228** 685
[18] Grimech H and Khater A 1995 *Surf. Sci.* **323** 198
[19] Virlouvet A 1998 *PhD Thesis* Le Mans, France
[20] Tigrine R, Khater A, Belhadi M and Rafil O 2005 *Surf. Sci.* **580** 1